Clim. Past Discuss., https://doi.org/10.5194/cp-2018-115
Manuscript under review for journal Clim. Past
Discussion started: 24 September 2018

Climate of the Past Discussions

Role of the stratospheric chemistry-climate interactions in the hot climate conditions of the Eocene

Sophie Szopa[1], Rémi Thiéblemont[1], Slimane Bekki [2], Svetlana Botsyun[1*], Pierre Sepulchre[1]

[1]Laboratoire des Sciences du Climat et de l'Environnement, LSCE-IPSL, CEA-CNRS-UVSQ, Gif-sur-Yvette, France.
[2]Laboratoire, Milieux, Observations Spatiales, Institut Pierre Simon Laplace, CNRS, Paris, France.
*Now at Department of Geosciences, University of Tübingen, Germany

Draft preparation for *Climate of the Past*

Correspondence to: Sophie Szopa (sophie.szopa@lsce.ipsl.fr)

Abstract

The stratospheric ozone layer plays a key role in atmospheric thermal structure and circulation. Although stratospheric ozone distribution is sensitive to changes in composition and climate, the modifications of stratospheric ozone are not usually considered in climate studies at geological time scales. Here, we evaluate with a chemical-climate model the potential role of stratospheric ozone chemistry in the case of the Eocene hot conditions. We show that the structure of the ozone layer is significantly different under these conditions ($4xCO_2$ climate and high concentrations of tropospheric N_2O and CH_4). While at mid and high latitudes, the total column ozone is found to be enhanced, the tropical ozone column remains more or less unchanged. These ozone changes are related to the stratospheric cooling and an acceleration of stratospheric Brewer-Dobson circulation simulated under Eocene climate. The meridional distribution of the total ozone column appears also to be strongly modified, showing particularly pronounced mid-latitudes maxima and steeper negative poleward gradient from these maxima. These anomalies are consistent with changes in the seasonal evolution of the polar vortex during the winter, especially in the Northern Hemisphere. Compared to a pre-industrial atmospheric composition, the changes in local ozone concentration reach up to 40% for zonal annual mean and affect temperature by a few Kelvins in the middle stratosphere.

As inter-model differences in simulating the deep past temperatures are quite high, the consideration of atmospheric chemistry, which is computationally demanding in Earth system models, may seem superfluous. However, our results suggest that using stratospheric ozone calculated by the model (and hence more physically consistent with Eocene conditions) instead of the commonly specified preindustrial ozone distribution can change the simulated global surface air temperature by 14%. This error is of the same order as the effect of non-CO_2 boundary conditions (topography, bathymetry, solar constant & vegetation). Moreover, the results highlight the sensitivity of stratospheric ozone to hot climate conditions. Since the climate sensitivity to stratospheric ozone feedback largely differs between models, it must be better constrained not only for deep past conditions but also for future climates.

Clim. Past Discuss., https://doi.org/10.5194/cp-2018-115
Manuscript under review for journal Clim. Past
Discussion started: 24 September 2018

1 Introduction

The absorption of incoming solar ultraviolet (UV) radiation by the stratospheric ozone is responsible for the heating of the stratosphere and hence its dynamical stability. In addition, this absorption is essential to the development of life because it prevents these very harmful UV radiations from reaching the Earth's surface. Stratospheric ozone is thus a key component of the radiative equilibrium and habitability of the Earth (Brasseur & Solomon, 2005). However, although deep time climates are more and more investigated with numerical climate models, the role of the stratosphere in such climates is usually neglected (e.g. Kageyama et al. 2017, Lunt et al. 2017).

The present-day stratosphere has been intensively studied to understand, anticipate and mitigate the global ozone depletion caused by the emissions of anthropogenic halogenated compounds such as chlorofluorocarbons and halons in the second part of the 20th century (WMO, 2014). The phasing out of the emissions has led to the start of a stratospheric ozone recovery since the end of the 90's (Chipperfield et al., 2017). However, in the context of increasing levels of greenhouse gases (e.g. GHGs such as CO_2, N_2O, and CH_4) and associated climate changes, the sensitivity of stratospheric ozone to other drivers, especially climate-related drivers, is increasingly investigated. For example, stratospheric ozone is sensitive to changes in N_2O, CH_4 and water vapour levels. N_2O enters in the stratosphere at the tropical tropopause and controls the levels of NOx, which are the most efficient ozone-destroying radicals in the middle stratosphere. Enhanced CH_4 levels lead to increase ozone production in the troposphere and lower stratosphere but also to increase water vapor levels which tend to favour ozone destruction (Revell et al. 2012, Bekki et al. 2011). An increase in CO_2 concentration results in a cooling of the stratosphere, which slows down ozone destruction in the upper stratosphere and hence favours ozone recovery in this region.

In addition to stratospheric chemical changes, the on-going climate change tends to intensify the large-scale stratospheric overturning circulation (the so-called Brewer-Dobson circulation), which is responsible of upward transport of air in the tropics and, poleward and downward transport at middle and high latitudes (see e.g. Butchart (2014) and references therein). These circulation changes result in reduced ozone levels in the tropical lower stratosphere due to the faster ascent of air in the lower tropical stratosphere (Avallone and Prather 1996) and enhanced ozone levels at middle and high latitudes (Bekki et al. 2011). This illustrates how stratospheric ozone responds to climate change. More recently, Chiodo et al. (2018) presented an analysis of the stratospheric ozone layer response to an abrupt quadrupling of CO_2 concentration in 4 chemistry climate models. As found previously (see e.g. WMO, 2014), they showed that increased CO_2 levels in the 4 models lead to a decrease in ozone concentration in the tropical lower stratosphere and an increase at high latitudes and in the upper stratosphere. However, there were large differences between models in the magnitude of the ozone response.

At the same time, stratospheric ozone changes also influence the climate. For instance, climate models have to account for the formation of the stratospheric ozone hole to be able to reproduce correctly the trends in Antarctic surface temperatures observed during the last half century (e.g. Son et al., 2010; McLandress et al., 2011;). Considering larger climate perturbations, Nowack et al. (2015) performed an abrupt $4xCO_2$ experiment with a comprehensive ocean-atmosphere-chemistry-climate model and found that neglecting stratospheric ozone changes triggered by CO_2 increase (i.e. specifying a

fixed ozone climatology in the model) led to overestimate the surface global mean temperature response by about 1K (i.e. 20% of the total surface temperature response). Chiodo & Polvani (2017) carried out the same numerical experiment ($4xCO_2$) with a different chemistry-climate model and found that, in contrast to Nowak et al. results, stratospheric ozone changes played a negligible role in the global surface temperature response. Nonetheless, they found that the stratospheric ozone feedback in their model significantly reduced the CO_2-induced poleward shift of the mid-latitude tropospheric jet by lowering the strength of the meridional temperature gradient near the tropopause. These results suggest that stratospheric ozone perturbations should be accounted for in climate models in order to fully capture the climate response to GHGs changes.

In the past of the Earth, the oxygenated atmosphere has encountered hot climatic conditions due to strong greenhouse effects. During the early Eocene (~ 56-50Ma) terrestrial temperatures at high latitudes were possibly up to 20 K higher than modern ones (e.g. Huber & Caballero, 2011). Under such a warm climate, biogenic emissions of N_2O and CH_4 were likely to be drastically boosted, being 4 to 5 times higher than the preindustrial ones (Beerling et al., 2011). Note however that, in most studies of deep past climates based on numerical climate models, the role of non-CO_2 gases is neglected (e.g. Deep MIP, Lunt et al. 2017). Beerling et al. (2011) studied the tropospheric chemical composition under a warm climate and potentially high biogenic emissions of the early Eocene (55 Ma). Using an Earth System Model including tropospheric chemistry, they found that the OH concentration, which is the main oxidant for most compounds in the troposphere, was significantly reduced (by 14 to 50%) due to higher levels of compounds to oxidize. The high tropospheric levels of reactive greenhouse gases (N_2O, CH_4 and O_3) were maintained under these conditions. Considering the full Earth System interactions, and in particular albedo change due to melting of continental snow, Beerling et al. (2011) calculated an increase of 1.4 to 2.7K in surface temperatures due to tropospheric chemical composition changes for the Eocene. However, since their model did not include stratospheric chemistry, they could not study stratospheric composition changes. Unger & Yue (2013) investigated the chemistry-climate feedbacks in the mid-Pliocene (~3 Ma) using a vegetation-chemistry-climate model simulating both stratospheric and tropospheric chemistry. This epoch is cooler than the Eocene but still of interest because its global climate is thought to be as warm as the climate projected for the end of the on-going century (+2-3 K compared to present-day). Compared to preindustrial conditions, the Unger & Yue (2013) model simulations indicated that the mid-Pliocene ozone burden was higher, by 25% in the troposphere and by 5% in the stratosphere. The global stratospheric ozone increase, resulting from a stronger tropical upwelling and a lower ozone destruction in the stratosphere, led to a 20% decrease in tropospheric ozone photolysis and hence OH production. As a consequence, tropospheric OH concentrations were reduced by 20-25% and hence the lifetime and burden of important reactive species (CO, CH_4) were significantly increased. Unger & Yue (2013) showed that the warming effect of the changes in chemically reactive compounds (i.e. CH_4, N_2O, tropospheric O_3) could have represented ~75% of the warming from CO_2 increase. The studies of Beerling et al. (2011) and Unger & Yue (2013) suggest that non-CO_2 greenhouse gases may have played a significant role in the overall climate in the Cenozoic greenhouse worlds.

Clim. Past Discuss., https://doi.org/10.5194/cp-2018-115
Manuscript under review for journal Clim. Past
Discussion started: 24 September 2018

As pointed out previously, most studies of the deep past climates assume that the atmospheric composition is fixed except for CO_2 because there is no estimate of these composition changes. The purpose of this paper is to investigate, using a stratospheric chemistry-climate model, to what extent the stratosphere, notably the ozone layer, might have been different in the early Eocene conditions and estimate the possible effects of these stratospheric changes on the tropospheric oxidizing capacity and climate. This epoch is characterized by high surface temperatures, elevated CO_2 levels, the absence of ice cap and a large extent of tropical vegetation. High CH_4 and N_2O levels are also expected based on Earth System Model simulations (Beerling et al. 2011). Whereas the data are sparse and have large uncertainties for the geological past, several proxy-based reconstructions of CO_2 levels and surface temperatures have been delivered, notably allowing to build an harmonised protocol for climate modelling of the early Eocene (Lunt et al. 2017) which will be used to intercompare climate model sensitivity during the on-going Paleoclimate Modelling Intercomparison Project (PMIP4). This protocol gathers recommendations on paleogeography, land cover, CO_2 and CH_4 concentrations, natural aerosols, solar constant and astronomical parameters but no recommendations have been provided yet for stratospheric conditions. In this work, we propose to examine the role of the stratospheric ozone layer in the Eocene climate. We first investigate the stratospheric ozone response to increased GHG levels such as the ones expected under the Eocene conditions by comparison to preindustrial climate conditions. We then discuss the methodology to account properly for these stratospheric ozone changes in deep time paleoclimate simulations. Finally, based on the model simulations, we estimate the difference in UV radiation reaching at Earth surface between this epoch and the preindustrial period and the resulting impact on tropospheric chemistry. The potential climate forcing of the stratospheric changes is also discussed.

2. Methodology

2.1 The LMDz-REPROBUS climate-chemistry model

Simulations are performed with the stratospheric chemistry-climate model developed in the framework of the IPSL-Earth System Model (IPSL-CM) development (Dufresne et al. 2013). The stratospheric chemistry is computed with the REPROBUS chemical model (Lefèvre et al. 1994, 1998, Jourdain et al. 2008) coupled with the LMDz atmospheric general circulation model (Hourdin et al. 2013). REPROBUS describes the chemistry of stratospheric source gases such as N_2O, CH_4, CH_3Cl, CH_3Br, and the associated radical chemistry of hydrogen, nitrogen oxides, chlorine, and bromine species. It computes the global distribution of trace gases, aerosols, and clouds within the stratosphere considering gas-phase and heterogeneous chemistry. The heterogeneous chemistry component takes into account the reactions on sulfuric acid aerosols, and liquid (ternary solution) and solid (Nitric Acid Trihydrate particles, ice) Polar Stratospheric Clouds (PSCs). The gravitational sedimentation of PSCs is simulated as well. The LMDz-REPROBUS chemistry-climate model allows an interactive coupling of ozone, shortwave heating rates and dynamics as recommended in Sassi et al. (2005). The resolution of the model is 3.75 degrees in longitude x 1.9 degrees in latitude and 39 vertical levels, with around 15 levels above 20 km and around 24 above 10km.

Clim. Past Discuss., https://doi.org/10.5194/cp-2018-115
Manuscript under review for journal Clim. Past
Discussion started: 24 September 2018

2.2 Simulation set-up

The setup of the four simulations performed in this study is summarized in Table 1. All the simulations consist of 30-year snapshots, starting from atmospheric physical conditions and surface temperatures taken from very long coupled atmosphere-ocean simulations. For the analysis of our chemistry-climate simulations, a 5-year spin-up is considered. For all the simulations, the solar constant is set to 1366Wm^{-2} and orbital parameters (obliquity, precession, and eccentricity) are set to modern values as recommended in the DeepMIP protocol (Lunt et al. 2017).

2.2.1 Preindustrial simulations

The boundary conditions of our preindustrial experiment (PREIND) include modern topography, land-sea mask, ice sheets and climatological mean values computed over the 1870-1899 period for sea surface temperatures (SSTs) and sea-ice extent. Greenhouse gases are set to preindustrial values, i.e. CO_2 level at 285 ppm, CH_4 level at 791 ppb, and N_2O level at 275 ppb. Halogenated ozone depleting substances of anthropogenic origin (i.e. fluorocarbons) are set to zero. Naturally emitted halogenated compounds (CH_3Br and CH_3Cl) are prescribed to their preindustrial levels (respectively, 7ppb and 482 ppb).

2.2.2 Eocene base case simulation

As for the PREIND experiment, the Eocene experiment (EOCENE) includes interactive chemistry which allows to calculate stratospheric composition. The physical boundary conditions for the EOCENE experiment (e.g. SSTs, sea-ice, land surface properties) are based on a climate simulation done with the fully coupled low-resolution climate model called FOAM (Jacob, 1997) and the LPJ dynamic global vegetation model (Sitch, 2003) coupled offline. The coupled ocean-atmosphere-vegetation simulation provides the surface conditions (SSTs, land surface conditions) required to simulate the climate with the LMDz atmospheric general circulation model. FOAM is forced with the Eocene paleogeography reconstruction of Herold et al. (2014). Compared to the present-day paleogeography, it includes major modifications, namely closed Drake and Tasman Seaways, an open Central American Seaway, and an open Parathetys Sea. Topography is altered as well, with lower Tibetan plateau and Andes. CO_2 is set to 1120 ppm, equivalent to 4x CO_2 preindustrial level ($[CO_2]_{PI}$), as Eocene CO_2 estimates range between 400 and 2400ppm (as reported by Lunt et al. (2017) based on boron isotopes analysis from Anagostou et al. 2016). This CO_2 value lies in the low-end of the Eocene compatible GHG forcing ranges, in particular those recommended by the DeepMIP project which proposes to test 3x$[CO_2]_{PI}$, 6x$[CO_2]_{PI}$ and 12x$[CO_2]_{PI}$ (Lunt et al. 2017). After 2,000 model years, SSTs simulated by FOAM are averaged over the last 100-year period to build a 12-month (seasonally varying) climatology used as a boundary condition for LMDz. FOAM coupling with the LPJ vegetation model provides an equilibrated vegetation as well, whose albedo and rugosity are extracted to serve as continental boundary conditions for LMDz.

Applying a coupled vegetation-atmosphere to the particularly warm climate of the early Eocene (55Ma), Beerling et al. (2011) have estimated that CH_4 and N_2O concentrations should have been much higher than nowadays and could have lied in

Clim. Past Discuss., https://doi.org/10.5194/cp-2018-115
Manuscript under review for journal Clim. Past
Discussion started: 24 September 2018

the 2384-3614 ppb and 323-426 ppb ranges respectively. The direct climate impact of highly enhanced CH_4 and N_2O levels is somewhat accounted for by setting CO_2 to high level (1120ppm) in the radiative module in our atmospheric circulation model. Their chemical impacts on stratospheric composition, notably the ozone layer, should also be considered (e.g. Revell et al. 2012). In order to do so, CH_4 and N_2O surface concentrations are set to 3614ppb and 323ppb respectively in the chemistry module (REPROBUS).

2.2.3 Eocene simulations with prescribed stratospheric ozone

In addition to the EOCENE experiment in which stratospheric ozone is calculated interactively, two other Eocene simulations (EOCENE_OzRoyer, EOCENE_Oz1855) are performed in which different climatological ozone representations are specified instead of ozone being calculated interactively. The ozone climatology in the EOCENE_OzRoyer experiment is rather typical of the 80s ozone distribution. It originates from fits to the ozone profile from Krueger and Mintzner (1976) and variations with altitude and latitude of the maximum ozone concentrations and total ozone column from Keating and Young (1986). This OzRoyer ozone climatology was constructed by J.-F. Royer (CNRM, Meteo France) and implemented in the LMDz atmospheric circulation model in the 80's. The Oz1855 ozone climatology in the EOCENE_Oz1855 experiment is more representative of the preindustrial period. It is based on a 11-year mean climatology centred on 1855 derived from historical transient LMDz-REPROBUS simulations (Szopa et al. 2013). This ozone climatology is commonly used for the simulation of past climates with the LMDz model.

The comparison between EOCENE and PREIND experiments, which both include interactive chemistry of the stratosphere, allows us exploring and quantifying the impacts of Eocene warm climate on stratospheric circulation and composition (Section 3). Furthermore, by comparing EOCENE experiment with EOCENE_OzRoyer and EOCENE_Oz1855 experiments allows to assess the role of the stratospheric ozone representation on the climate response to Eocene extreme conditions (Section 4). Note that the statistical significance of anomaly fields is estimated here using a Student's t-test.

3. Impacts of Eocene conditions on stratosphere

3. 1 Stratospheric ozone in Eocene conditions

We first investigate the impact of Eocene conditions on stratospheric ozone with respect to preindustrial conditions. Figure 1 shows the latitude/pressure zonally average cross-sections of temperature, ozone and zonal wind anomalies associated with the Eocene conditions. As expected, the CO_2 increase leads to a global radiative cooling of the stratosphere with decreases in temperatures exceeding 12K above 10 hPa (~32 km) and a warming of the troposphere (Figure 1, left panel). The cooling of the stratosphere slows down the ozone destruction, resulting in an increase of stratospheric ozone concentrations (Haigh and Pyle, 1982). This is consistent with the statistically significant positive ozone anomalies found above 50 hPa (~20 km) over the polar regions and above 10 hPa in the tropical band (Figure 1, middle panel). Note that this effect increases with altitude

in the stratosphere as the photochemical control on ozone level becomes prominent (Brasseur and Solomon, 2005). Similarly to the results of Chiodo et al. (2018), a maximum ozone increase of ~40% is found at about 2-3 hPa (~40 km).

In contrast, the lower tropical stratosphere (30°S-30°N, 100-30 hPa) exhibits a statistically significant ozone decrease of up to 40%. In this region, the ozone concentration is mostly controlled by transport processes (Brasseur and Solomon, 2005), especially the strength of the Brewer-Dobson circulation ascending branch. Figure 1 (right panel) shows the age of air (AoA) at 36 hPa, calculated after 20 years of simulations by taking as a reference entry point the equatorial lowermost stratosphere, slightly above the tropopause (i.e. pressure level corresponding to 74 hPa). Globally, the stratospheric AoA is younger in the Eocene experiment than in the preindustrial one, revealing an acceleration of the Brewer-Dobson circulation under Eocene conditions. This, in turn, is consistent with the reduced ozone concentration in the lower tropical stratosphere. Note also that the tropopause height is globally lifted up in the Eocene experiment (not shown). The rise of the tropopause is a robust feature of warmer climate conditions (Sausen and Santer, 2003) and contributes to the negative ozone anomaly found in the vicinity of the tropopause region (Figure 1, middle panel) (Dietmüller et al. 2014).

Next, we examine anomalies of the annual total ozone column (TOC). Figure 2 shows the comparison of the latitudinal distribution of the annual TOC for Eocene and Preindustrial conditions. In both simulations (Figure 2, top panel), the TOC shows a minimum in the tropical region [20°S, 20°N] of ~270 Dobson unit (DU) and maxima near 55°N and 55°S, followed by poleward decreases that are more pronounced in the Southern Hemisphere. The differences between Eocene and preindustrial conditions (Figure 2, bottom panel) reveal no changes in the tropical band 20°S-20°N, but statistically significant positive anomalies at mid-latitudes and in polar regions. The mid-latitude maxima reach ~390 DU for preindustrial conditions, whereas they exceed 430 DU for Eocene conditions. This TOC anomalies latitudinal distribution is overall consistent with projections of TOC anomalies simulated in response to the 21st climate change post-CFC era (Li et al., 2009) or to an abrupt 4xCO_2 increase from preindustrial climate conditions (Chiodo et al., 2018). The detailed comparison of our results with those of Chiodo et al. (2018) shows, however, noticeable differences at high latitudes. In our simulations, the TOC anomalies peak at 45° S and 50° N with maximum differences of 50 and 60 DU, respectively; the anomalies decrease from these maxima to about 30 DU at high latitudes (Figure 2, top panel). In Chiodo et al. (2018), hints of such a decrease was found in the Southern Hemisphere for only two out of the four models that are inter-compared, and no such decrease was seen in the Northern Hemisphere. The negative poleward TOC gradient at high latitudes appears to strengthen markedly under Eocene conditions in the Northern Hemisphere (Figure 2, top panel). The seasonal dependence of the TOC high-latitudes poleward gradient for the Eocene and preindustrial conditions in the Northern Hemisphere is explored on Figure 3. Figure 3 reveals that, under Eocene conditions, the negative gradient is particularly pronounced during the winter season (from October to March), when the stratospheric polar vortex dominates the high latitudes circulation in the Northern Hemisphere. Hence, this indicates substantial changes in the stratospheric circulation associated with the Eocene conditions that we examine further in section 3.2.

Clim. Past Discuss., https://doi.org/10.5194/cp-2018-115
Manuscript under review for journal Clim. Past
Discussion started: 24 September 2018

3. 2 Stratospheric circulation in Eocene conditions

In order to detect possible changes in the strength of the polar vortex, the anomalies of the zonal-mean zonal wind are analysed and shown on Figure 4. In the Eocene experiment, the high latitudes stratospheric westerlies maxima, indicative of the average location of the core of the stratospheric Southern and Northern Hemisphere polar night jets (near 60° S and 60° N), appear to be overall stronger and also shifted equatorward in comparison with the preindustrial climatology (black contour). These results suggest a strengthening and an extension of stratospheric polar vortices. Note also that the upward extension of the subtropical upper tropospheric jets in both hemispheres (centred near 35°N/S around 200 hPa) are consistent with the tropopause rising associated with Eocene conditions.

Figure 5 shows the seasonal evolution of the zonal-mean zonal wind near the climatological location of the core of the stratospheric polar night jet in the Northern hemisphere (i.e. 60°N and 10 hPa). Regardless of simulated climate conditions, the winter season (September to April) is characterized by strong westerlies associated with the formation and development of the Arctic polar vortex, and by a large inter-annual variability driven by the planetary wave activity that propagate from the troposphere and drag the stratospheric mean flow by wave breaking (Andrews et al., 1987). Note that the inter-annual variability increases progressively over the winter season and becomes particularly large after December. This evolution indicates a transition from a radiatively controlled state in early winter (i.e. radiative heating difference between the tropics and the pole) to a dynamical phase where the easterly momentum forcing of planetary waves on the mean flow becomes prominent (e.g. Kodera and Kuroda, 2002). The summer season (May to August) is dominated by radiatively controlled weak easterlies, that inhibit the propagation of planetary waves. The inter-annual variability in summer is therefore strongly reduced.

The comparison between the two simulations reveals that under the Eocene conditions, the amplitude of the zonal-mean zonal wind seasonal cycle is much larger than under preindustrial conditions. The polar night jet westerlies are 2 times stronger during the Eocene winter than the preindustrial winter, with an average peak of ~70 m/s in January for the Eocene simulation against a ~35 m/s peak in December for the PREIND simulation. Furthermore, in the Eocene simulation, the persisting low inter-annual variability in early winter suggests that the transition between the radiative and the dynamical phases is delayed compared to the PREIND simulation. In contrast, in summer, the amplitude of easterlies is similar in both simulations. These differences in the seasonal evolution of the zonal-mean zonal wind are consistent with the seasonal evolution of the ozone gradient shown on Figure 3. Indeed, under Eocene conditions, the stronger winter polar vortex is associated with a reinforcement of the mixing barrier at its edge. This leads in turn to a reduction of air exchanges between mid- and polar latitudes and hence to a steepening of the poleward ozone gradient. Similar (though less pronounced) differences between Eocene and preindustrial conditions are found in the Southern Hemisphere (not shown).

To understand the difference in the seasonal evolution of the stratospheric zonal flow between the preindustrial and Eocene conditions, we examine the mid-stratosphere poleward temperature gradient from 30° N and 70° N and the lower stratosphere mid-latitudes eddy heat flux in both simulations (Figure 6). The poleward temperature gradient partly drives the

Clim. Past Discuss., https://doi.org/10.5194/cp-2018-115
Manuscript under review for journal Clim. Past
Discussion started: 24 September 2018

strength of the zonal wind via the thermal wind balance relationship (Holton, 2004), whereas the eddy heat flux at 100 hPa is an index of the planetary wave activity entering the stratosphere and hence affecting the strength of the polar vortex (Newman et al., 2001). The heat flux is expressed as $\langle v'T' \rangle$, where primes denote the deviation from the zonal mean (i.e. also referred to as "eddies") of the meridional wind v and the temperature T; the brackets denote the zonal mean.

In JJA period, the positive poleward temperature gradient (Figure 6, top panel), directly caused by latitudinal differences in the ozone shortwave heating, leads to the large scale easterly flow (Figure 5). According to the Charney-Drazin criterion, this in turn prevents planetary waves to enter the stratosphere as revealed by the near zero heat flux values (Figure 6, bottom panel). Note that the summer values of the poleward temperature gradient, the eddy heat flux and the zonal-mean zonal wind are very close in both simulations. They start diverging in early winter. For the Eocene conditions, the negative poleward temperature gradient exhibits a larger decrease, which is, by December, twice as large as the one found for the preindustrial conditions (Figure 6, left panel). This difference is consistent with higher CO_2 concentrations in the EOCENE simulation, which lead to a stronger stratospheric radiative cooling during the polar night compared to the PREIND simulations, and hence to the development of a stronger polar vortex in early winter (Figure 5). The stronger polar vortex is also consistent with reduced planetary wave activity in early winter under Eocene conditions (Figure 6, bottom panel). The planetary wave activity increases considerably in mid-winter, peaking in January and February for PREIND and EOCENE simulations, respectively. This increase is accompanied by a decline of the negative poleward temperature gradient (Figure 6, top panel), by an average decrease of the zonal-mean zonal wind and by an increase of its inter-annual variability (Figure 5). The polar vortex weakening is more abrupt under Eocene conditions, which is consistent with the larger wave activity in mid- to late-winter. Finally, note that the 1-month lag of the heat flux peak in Eocene simulation compared to the Preindustrial simulation is consistent with the delayed transition between the radiative and the dynamical phases mentioned above.

4. Climate impact of an interactive stratospheric chemistry

Model results shown in the previous section suggest that stratospheric dynamics and composition were very significantly altered under Eocene hot conditions in comparison with pre-industrial climate conditions. In turn, these stratospheric changes may also have influenced the establishment of the Eocene climate. Nowack et al. (2015) have shown that stratospheric changes driven by ozone changes can have an impact on the climate sensitivity in the context of high GHG concentrations for present day conditions. The importance of this stratospheric ozone-climate feedback has, however, not been assessed in the context of Eocene hot climate. In this section, we estimate the role of this feedback on the overall Eocene climate response by comparing the EOCENE experiment (i.e. where ozone is calculated interactively and, hence, is physically consistent with Eocene conditions) with Eocene_OzRoyer and Eocene_Oz1855 experiments (i.e. where pre-industrial ozone climatologies are prescribed in Eocene simulations). The latter simulations follow the protocol usually recommended for simulating paleo climates (e.g. Kageyama et al., 2017).

Clim. Past Discuss., https://doi.org/10.5194/cp-2018-115
Manuscript under review for journal Clim. Past
Discussion started: 24 September 2018

Table 2 shows the total ozone and temperature changes as well as the effective radiative forcings induced by the use of an interactive stratospheric chemistry instead of seasonally varying prescribed climatologies. All the results in this section are discussed in term of 25-year mean. The effective radiative forcing is computed as the difference of net radiative flux at the top of atmosphere (TOA) between two atmospheric simulations (with ozone calculated interactively – with ozone climatology) as defined in Fig 8.1.d of Myhre et al. (2013).

Figure 7 shows the distribution of total ozone column as a function of latitudes for the different configurations. The preindustrial ozone distribution computed by REPROBUS and the Szopa et al. (2013) ozone climatology are represented as well. Comparing only the different preindustrial ozone distributions, the TOC in the experiment with interactive calculation of ozone (PREIND in black) is higher than those of the climatologies (OzRoyer in blue, Oz1855 in brown). In addition, the interactive calculation of Eocene ozone (EOCENE in red) leads to much higher TOC than in the preindustrial climatologies (blue, brown), in the 2000 climatology (green) and in the preindustrial interactive ozone simulation (black). The global mean TOC is increased by about 45 DU or 35 DU with respect to the preindustrial OzRoyer or Oz1855 climatologies respectively. For the sake of comparison, the global mean TOC had decreased by about 13 DU only between the 1960's and the end of 90's because of the past emissions of anthropogenic halogenated compounds, and the expected TOC increase at the 2100 horizon is projected to be between 13 and 32 DU depending on future anthropogenic emissions of GHGs (Bekki et al. 2013, Szopa et al. 2013). Taking the ozone distribution calculated in the EOCENE simulation as the reference, the TOC bias in an inappropriate ozone climatology can be 2 times higher (in the case of the OzRoyer climatology) than the TOC change calculated by the model between Eocene and preindustrial conditions (EOCENE versus PREIND, see section 3).

The TOC difference between the EOCENE ozone distribution and ozone climatologies peak at mid latitudes (about 40°), reaching almost 70 DU for the Oz1855 climatology and about 100 DU for the OzRoyer climatology (Fig. 8, left). In order to identify the regions responsible for the general increase in TOC calculated from pre-industrial to Eocene conditions, the zonal mean distribution of ozone difference between EOCENE and Oz1855 climatologies are plotted in DU/km on the Fig.8 (right panel). The TOC increase in EOCENE is largely due to an enhancement in ozone in the upper stratosphere. The TOC change in the tropics are very moderate because the upper-stratospheric ozone enhancements are more or less compensated by lower stratospheric ozone decreases brought about by the acceleration of the Brewer-Dobson circulation, namely the faster ascent in the tropics (section 3). TOC enhancements peak at mid-latitudes because the ozone concentration increases reach down to the 150 hPa at mid-latitudes, again certainly linked to the acceleration of the Brewer-Dobson circulation and more specifically the faster descent at mid- and high latitudes. Below 200 hPa, around the tropopause region, extra-tropical EOCENE ozone concentrations are lower than in Oz1855 climatology, mostly because of the rise in the tropopause height (section 3).

Ozone changes naturally lead to temperature changes, especially in the stratosphere where ozone and temperature are closely coupled. Figure 9 shows the zonal mean distribution of temperature difference between EOCENE and EOCENE_Oz1855 simulations. The impact is weak below 400 hPa since SSTs are fixed and identical in all the Eocene simulations (EOCENE, EOCENE_OzRoyer, EOCENE_Oz1855). The change in zonal mean temperatures below 400 hPa does not exceed 0.15 K,

Clim. Past Discuss., https://doi.org/10.5194/cp-2018-115
Manuscript under review for journal Clim. Past
Discussion started: 24 September 2018

but can almost reach 0.5 K for the northern polar latitudes when the interactive ozone simulation (EOCENE) is compared to the EOCENE_OzRoyer (not shown). In contrast, temperatures above about 200 hPa are significantly impacted by the choice of ozone distribution used in the model. Temperatures are more than 2.5 to 3 K higher at middle and high latitudes in both hemispheres when ozone is calculated interactively instead of using the preindustrial 1855 climatology. The largest differences are found in the polar stratosphere where temperatures are 4.5 K higher at ~130 hPa and for middle stratospheric tropical temperatures at ~60 hPa that are 3.5 K lower in the simulation with interactive ozone compared to the one with the pre-industrial climatology.

5. Do we need to consider stratospheric ozone feedback in deep past simulations?

5.1 Impact on climate

The consideration of a stratospheric ozone compatible with the Eocene conditions perturbs the radiative balance compared to the use of a preindustrial climatology. The net radiative change (shortwave + longwave) between the simulation with interactive chemistry and the simulation with pre-industrial climatology corresponds to a 1.7 $W.m^{-2}$ effective radiative forcing. This radiative forcing from the stratospheric ozone response represents a positive climate feedback which is commonly ignored in Eocene climate simulations. In order to estimate the potential impact of an interactive ozone on surface temperature under the Eocene conditions, we consider a large range of climate sensitivity from 0.4 to 1.2 $K.W^{-1}.m^2$ (Knutti et al., 2017). Given such a broad range, the surface temperature response to this stratospheric forcing could range from 0.7 to 2.0 K (assuming an effective radiative forcing of 1.7 $W.m^{-2}$). The surface temperature response to a specific radiative forcing depends on the considered climate conditions and on the nature of the climate forcer. Considering an interactive stratospheric ozone chemistry under a $4xCO_2$ climate perturbation, Nowak et al. (2014) found a climate sensitivity of 1.05 $K.W^{-1}.m^2$ in their Earth System model. Applying this climate sensitivity, the surface temperature change associated with the ozone feedback would be about 1.8 K when considering interactive stratospheric chemistry (compared with the EOCENE_Oz1855 run). The climate sensitivity to ozone change can obviously vary from one Earth System Model to another since, for example, the sensitivity of the Brewer Dobson circulation to climate is highly model-dependant (SPARC CCMVal, 2010). Nonetheless, this estimation allows us to discuss the importance of considering this chemistry-climate feedback when attempting to simulate past hot climates. According to the IPCC AR5 report, the global land surface air temperature anomaly is +12.7 K for the Early Eocene Climatic Optimum (Masson-Delmotte et al., 2013). This estimation is based on the simulations from several models analysed by Lunt et al. (2012) for which there was no common modelling protocol (e.g. CO_2 being in the PIx2 to PIx16 range). One of these models, the HadCM model, estimates that the effect of changing non-CO_2 boundary conditions (topography, bathymetry, solar constant and vegetation) for Eocene conditions leads to a 1.8 K increase in the global mean surface air temperature (to be compared to a 3.3 K increase when doubling the CO_2). The feedback of stratospheric ozone on surface air temperature could thus represent about 15% of the

total temperature anomaly reported between Eocene and preindustrial conditions and be as important as the effect of external forcings.

In strong greenhouse climate, the terrestrial carbon and nitrogen cycles are intensified, releasing high CH_4 and N_2O in the atmosphere (Beerling et al. 2011). The effect of changing N_2O and CH_4 in the troposphere (including the H_2O increase in the stratosphere induced by the CH_4 increase) has been assessed by Beerling et al. (2011). These authors find, with the STOCHEM model, a 2.1K increase of global surface temperature due solely to the tropospheric composition changes. Our results suggest that the effect of the stratospheric ozone feedback on surface temperatures is of similar importance.

5.2 Impact on tropospheric conditions

Using an Earth System Model including chemistry, Unger & Yue (2013) found that under warm Pliocene conditions (suspected to be due to high CH_4 levels), the stratospheric ozone burden was 5% higher than the preindustrial one. This stratospheric ozone increase resulted in a 20% reduction in the tropospheric photolysis rate of ozone (O_3 +hv -> O^1D + O_2) that leads to the formation of OH, the hydroxyl radical. This radical is the main oxidant of the troposphere and its decrease (of 20 to 25% in the Unger and Yue simulations) impacts the lifetime of chemical species and in particular CH_4. Our simulations show a 7.2% increase of the stratospheric ozone burden when comparing the EOCENE and the PREIND simulation (both including interactive chemistry) and a 8.8% difference when comparing the EOCENE simulation to the EOCENE_Oz1855.

In addition, we estimate the change in surface UV radiations and ozone photolysis in the Eocene conditions. Using the Radiation transfer model Quick TUV Calculator with a Pseudo-spherical discrete ordinate 4 streams (http://cprm.acom.ucar.edu/Models/TUV/Interactive_TUV/), we estimate the effect of the stratospheric ozone increase on the ozone photolysis which controls the OH production. Considering a 65 DU change at a 50° latitude (corresponding to the maximum of Fig. 8), the photolysis rate at the surface decreases by 25%. A decrease in the ozone photolysis rate would induce a significant decrease in OH and hence in the tropospheric oxidizing capacity, thus making CH_4 longer lived and reinforcing its effect on climate. It would also impact the overall tropospheric chemistry.

6. Conclusion

The stratospheric dynamics and ozone layer respond to - and interact with - atmospheric variations (climate, tropospheric GHG content). In this study, we simulate these interactions in the case of the hot Eocene climate using a chemistry-climate model. We characterize the changes in ozone and middle atmospheric dynamics induced by a $4xCO_2$ climate and by elevated concentrations of CH_4 and N_2O. The climate impact of the stratospheric response under hot conditions is also estimated.

Comparing the Eocene simulation with a preindustrial simulation, we find a sharp increase in ozone in the upper stratosphere (reaching 40% at 2-3hPa in the tropics) linked to the strong cooling of the stratosphere (up to -12 K at 10 hPa) which slows down the chemical destruction of ozone. Meanwhile, ozone is greatly reduced in the lower tropical stratosphere (up to 40%)

due to the intensification of Brewer Dobson circulation. These results are in agreement with previous modelling studies that considered current tropospheric composition and a $4xCO_2$ climate change.

As a consequence of the opposite ozone changes in the tropics (enhanced ozone in the upper stratosphere, reduced ozone in the lower stratosphere), the tropical Total Ozone Column (TOC) is not affected much by the difference in climate between the Eocene and pre-industrial periods. On the contrary, at mid-latitudes and, to a lesser extent, in the polar regions, the TOC is considerably increased. The TOC meridional distribution is also strongly modified, exhibiting particularly pronounced mid-latitudes maxima and steeper negative poleward gradient from these maxima. These meridional distribution changes reflect significant polar vortex changes during the winter/early spring, especially in the Northern Hemisphere. The polar vortex becomes stronger and more extended equatorward under the Eocene conditions, thus isolating the polar vortex from the mid-latitudes. In our simulations, this reinforcement of the polar vortex under Eocene conditions is consistent with the cooling of the upper stratosphere in high CO_2 climate and the reduced intensity of the planetary waves activity in early winter.

We then explore the possible role of the stratospheric ozone response in the establishment of the Eocene climate. For that purpose, we compare the simulations with interactive ozone with simulations forced by the use of preindustrial ozone climatologies. The difference in global mean TOC between the Eocene simulation and simulations using preindustrial climatologies is two to three times higher than the change in ozone observed between 1960 and end of the 90s (the minimum TOC) and of the same order as the changes projected between 2000 and 2100. The ozone increase in the upper stratosphere in the case of Eocene interactive ozone warms the atmosphere by up to 3 K above 230 hPa. In the tropical lower stratosphere, zonal mean temperatures are up to 3.5 K lower for the Eocene stratospheric ozone compared to the preindustrial ozone. These changes in the thermal structure of the middle atmosphere could, via atmospheric circulation teleconnections, have significant regional consequences. Using the sensitivity of surface temperatures to stratospheric ozone changes determined by Nowak et al. 2014 (though climate sensitivity varies among climate-chemistry models), we estimate the contribution of stratospheric ozone feedback to surface temperature change in Eocene hot climate simulations. We find that it is potentially as important as the uncertainties due to non-CO_2 boundary conditions (topography, bathymetry, solar constant & vegetation) or to gaseous tropospheric chemistry. The results also highlight some of the limitations in using present-day ozone climatologies for deep time climate simulations.

Author contributions. The idea of the study, the design of numerical simulations and the radiative forcing analysis come from S. Szopa. R. Thiéblemont performed all the analysis on atmospheric dynamics. S. Botsyun provided the Eocene boundary conditions. S. Szopa & R. Thiéblemont prepared the first draft of the manuscript. All co-authors contributed to its edition.

Acknowledgements. This work is supported by a grant from the French National Research Agency (ANR-16-CE31-0010 for the PALEOx project). This work was granted access to the HPC resources of TGCC under the allocation 2017-A0050102212 made by GENCI (Grand Equipement National de Calcul Intensif). The authors are thankful to the NCAR

Atmospheric Chemistry Division (ACD) for the distribution of the NCAR/ACD TUV: Tropospheric Ultraviolet & Visible Radiation Model (URL: http://cprm.acd.ucar.edu/Models/TUV/) and the availability of their quicktool. We thank Y. Donnadieu for preparing the paleogeographical conditions for Eocene simulations and Marion Marchand for her advice in the use of the REPROBUS model.

References

Anagnostou, E., John, E., Edgar, K., Foster, G., Ridgwell, A., Inglis, G., Pancost, R., Lunt, D., and Pearson, P.: Changing atmospheric CO2 concentration was the primary driver of early Cenozoic cli- mate, Nature, 533, 380–384, doi:10.1038/nature17423, 2016.

Andrews, D. G., J. R. Holton, and C. B. Leovy, 1987: Middle Atmospheric Dynamics. Academic Press, 489 pp.

Avallone LM, Prather MJ. Photochemical evolution of ozone in the lower tropical stratosphere Journal of Geophysical Research: Atmospheres. 101: 1457-1461. DOI: 10.1029/95JD03010, 1996.

Beerling D. J. et al. Enhanced chemistry-climate feedbacks in past greenhouse worlds, Proc. Natl. Acad. Sci. USA, vol. 108, no. 2, p9770–9775 /doi/10.1073/pnas.1102409108, 2011.

Bekki S. & G.E. Bodeker (Coordinating Lead Authors) A.F. Bais N. Butchart V. Eyring D.W. Fahey D.E. Kinnison U. Langematz B. Mayer R.W. Portmann E. Rozanov, P. Braesicke A.J. Charlton-Perez N.E. Chubarova I. Cionni S.B. Diaz N.P. Gillett M.A. Giorgetta N. Komala F. Lefèvre C. McLandress J. Perlwitz T. Peter K. Shibata, Future Ozone and Its Impact on Surface UV, Chapter 3 in *Scientific Assessment of Ozone Depletion: 2010*, Global Ozone Research and Monitoring Project–Report No. 52, 516 pp., World Meteorological Organization, Geneva, Switzerland, 2011.

Bekki S., Rap A., Poulain V., Dhomse S., Marchand M., Lefèvre F., Forster P. M., Szopa S., Chipperfield M. P. (2013) Climate impact of stratospheric ozone recovery. Geophysical Research Letters, American Geophysical Union, 2013, 40 (11), pp.2796-2800.

Brasseur, Guy P.; Solomon, Susan, Aeronomy of the Middle Atmosphere: Chemistry and Physics of the Stratosphere and Mesosphere,. 644 p. 3rd rev. and enlarged ed. Springer, 2005.

Butchart N. (2014): The Brewer-Dobson circulation. Reviews of Geophysics, https://doi.org/10.1002/2013RG000448

Chiodo, G., and L.M. Polvani (2017): Reduced Southern Hemispheric circulation response to quadrupled CO2 due to stratospheric ozone feedback, Geophysical Research Letters, 44, 465–474, DOI:10.1002/2016GL071011.

Chiodo, G., L.M.Polvani, D.R.Marsh, A.Stenke, W.Ball, E.Rozanov, S.Muthers, and K.Tsigaridis (2018): The response of the ozone layer to quadrupled CO2 concentrations, Journal of Climate, DOI:10.1175/JCLI-D-17-0492.1

Chipperfield M. P., S. Bekki, S. Dhomse, N. R. P. Harris, B. Hassler, R. Hossaini, W. Steinbrecht, R. Thiéblemont & M. Weber (2017): Detecting recovery of the stratospheric ozone layer. Nature volume 549, pages 211–218.

Dietmüller, S., M. Ponater, and R. Sausen, 2014: Interactive ozone induces a negative feedback in CO2-driven climate change simulations. *J. Geophys. Res. Atmos*., 119, 1796–1805, https:// doi.org/10.1002/2013JD020575.

Dufresne J-L et al. Climate change projections using the IPSL-CM5 Earth System Model: from CMIP3 to CMIP5. Clim. Dynamics , 40(9-10), pp. 2123-2165, doi: 10.1007/s00382-012-1636-1, 2013.

Haigh, J. D. and Pyle, J. A.: Ozone perturbation experiments in a two-dimensional circulation model, Q. J. Roy. Meteorol. Soc., 109, 551–574, doi:10.1002/qj.49710845705, 1982.

Herold, N., Buzan, J., Seton, M., Goldner, A., Green, J. A. M., Müller, R. D., Markwick, P., and Huber, M.: A suite of early Eocene (~ 55 Ma) climate model boundary conditions, Geosci. Model Dev., 7, 2077-2090, https://doi.org/10.5194/gmd-7-2077-2014, 2014.

Holton, J. R., An introduction to dynamic meteorology, Elsevier Academic Press, Burlington, MA, pp. 535, 2004.Hourdin, F., Grandpeix, JY., Rio, C. et al. Clim Dyn (2013) 40: 2193. https://doi.org/10.1007/s00382-012-1343-y

Huber, M. and Caballero, R. The early Eocene equable climate problem revisited, Clim. Past, 7, 603-633, doi:10.5194/cp-7-603-2011, 2011.

Jacob, R., 1997, "Low Frequency Variability in a Simulated Atmosphere Ocean System", Ph.D. thesis, University of Wisconsin-Madison.

Jourdain, L., S. Bekki, F. Lott, and F. Lefèvre. The coupled chemistry-climate model LMDz-REPROBUS: description and evaluation of a transient simulation of the period 1980-1999, Ann. Geophys., 26, 1391-1413, 2008.

Kageyama, M., Albani, S., Braconnot, P., Harrison, S. P., Hopcroft, P. O., Ivanovic, R. F., Lambert, F., Marti, O., Peltier, W. R., Peterschmitt, J.-Y., Roche, D. M., Tarasov, L., Zhang, X., Brady, E. C., Haywood, A. M., LeGrande, A. N., Lunt, D. J., Mahowald, N. M., Mikolajewicz, U., Nisancioglu, K. H., Otto-Bliesner, B. L., Renssen, H., Tomas, R. A., Zhang, Q., Abe-Ouchi, A., Bartlein, P. J., Cao, J., Li, Q., Lohmann, G., Ohgaito, R., Shi, X., Volodin, E., Yoshida, K., Zhang, X., and Zheng, W.: The PMIP4 contribution to CMIP6 – Part 4: Scientific objectives and experimental design of the PMIP4-CMIP6 Last Glacial Maximum experiments and PMIP4 sensitivity experiments, Geosci. Model Dev., 10, 4035-4055, https://doi.org/10.5194/gmd-10-4035-2017, 2017.

Keating, G. M. and D. F. Young, 1985: Interim reference models for the middle atmosphere, Handbook for MAP, vol. 16, 205-229.

Knutti, R., Rugenstein, M. A. A., and Hegerl, G. C.: Beyond equilibrium climate sensitivity, *Nat. Geosci*., 10, 727–736, https://doi.org/10.1038/ngeo3017, 2017

Kodera, K., and Y. Kuroda (2002), Dynamical response to the solar cycle, J. Geophys. Res., 107(D24), 4749, doi:10.1029/2002JD002224.

Krueger, A. J. & Minzner, R. A., A Mid-Latitude Ozone Model for the 1976 U.S. Standard Atmosphere, J. Geophys. Res., 81, 4477, (1976).

Lefèvre, F. et al. Chemistry of the 1991-1992 stratospheric winter: Three-dimensional model simulations, J. Geophys. Res., 199, 8183-8195, 1994.

Lefèvre, F. et al. The 1997 Arctic ozone depletion quantified from three-dimensional model simulations, Geophys. Res. Lett., 25(13), 2425-2428, 1998.

Li, F., Stolarski, R. S., and Newman, P. A.: Stratospheric ozone in the post-CFC era, Atmos. Chem. Phys., 9, 2207-2213, https://doi.org/10.5194/acp-9-2207-2009, 2009.

Lunt D.J. et al. A model-data comparison for a multi-model ensemble of early Eocene atmosphere-ocean simulations: EoMIP. *Clim. Past*, 8, 1717-1736, doi:10.5194/cp-8-1717-2012, 2012.

Lunt, D. J., Huber, M., Anagnostou, E., Baatsen, M. L. J., Caballero, R., DeConto, R., Dijkstra, H. A., Donnadieu, Y., Evans, D., Feng, R., Foster, G. L., Gasson, E., von der Heydt, A. S., Hollis, C. J., Inglis, G. N., Jones, S. M., Kiehl, J., Kirtland Turner, S., Korty, R. L., Kozdon, R., Krishnan, S., Ladant, J.-B., Langebroek, P., Lear, C. H., LeGrande, A. N., Littler, K., Markwick, P., Otto-Bliesner, B., Pearson, P., Poulsen, C. J., Salzmann, U., Shields, C., Snell, K., Stärz, M., Super, J., Tabor, C., Tierney, J. E., Tourte, G. J. L., Tripati, A., Upchurch, G. R., Wade, B. S., Wing, S. L., Winguth, A. M. E., Wright, N. M., Zachos, J. C., and Zeebe, R. E.: The DeepMIP contribution to PMIP4: experimental design for model simulations of the EECO, PETM, and pre-PETM (version 1.0), Geosci. Model Dev., 10, 889-901, https://doi.org/10.5194/gmd-10-889-2017, 2017.

Masson-Delmotte V. et al. Information from Paleoclimate Archives. In: Climate Change 2013: The Physical Science Basis. Contribution of WG I to the Fifth Assessment Report of the IPCC [Stocker, T.F., et al. (eds.)]. Cambridge University Press, 2013.

McLandress, C., Shepherd, T. G., Scinocca, J. F., Plummer, D. A., Sigmond, M., Jonsson, A. I., and Reader, M. C.: Separating the Dynamical Effects of Climate Change and Ozone Depletion. PartII: Southern Hemisphere Troposphere, *J.Climate*, 24, 1850– 1868, https://doi.org/10.1175/2010JCLI3958.1, 2011

Myhre, G., D. Shindell, F.-M. Bréon, W. Collins, J. Fuglestvedt, J. Huang, D. Koch, J.-F. Lamarque, D. Lee, B. Mendoza, T. Nakajima, A. Robock, G. Stephens, T. Takemura and H. Zhang, 2013: Anthropogenic and Natural Radiative Forcing. In: Climate Change 2013: The Physical Science Basis. Contribution of Working Group I to the Fifth Assessment Report of the Intergovernmental Panel on Climate Change [Stocker, T.F., D. Qin, G.-K. Plattner, M. Tignor, S.K. Allen, J. Boschung, A. Nauels, Y. Xia, V. Bex and P.M. Midgley (eds.)]. Cambridge University Press, Cambridge, United Kingdom and New York, NY, USA.

Newman, P. A., Nash, E. R., & Rosenfield, J. E. (2001). What controls the temperature of the Arctic stratosphere during the spring. Journal of Geophysical Research,106, 19,999–20,010. https://doi.org/10.1029/2000JD000061.

Nowack, PJ, Abraham, NL, Maycock, AC, Braesicke, P, Gregory, JM, Joshi, MM, Osprey, A, Pyle, JA (2015). A large ozone-circulation feedback and its implications for global warming assessments, Nature Climate Change, Volume: 5, Issue: 1, Pages: 41-45, DOI: 10.1038/NCLIMATE2451.

Revell, L. E., Bodeker, G. E., Huck, P. E., Williamson, B. E., and Rozanov, E.: The sensitivity of stratospheric ozone changes through the 21st century to N_2O and CH_4, Atmos. Chem. Phys., 12, 11309-11317, https://doi.org/10.5194/acp-12-11309-2012, 2012.

Sassi F. et al. The effects of interactive ozone chemistry on simulations of the middle atmosphere, Geophys. Res. Lett., 32, L07811, doi:10.1029/2004GL022131, 2005.

Sausen, R. and Santer, B. D. (2003) Use of changes in tropopause height to detect influences on climate, Meteorol Z, 12(3), 131–136.

Sitch, S., et al. (2003), Evaluation of ecosystem dynamics, plant geography and terrestrial carbon cycling in the LPJ dynamic vegetation model, Global Change Biol., 9, 161–185.

Son, S.-W., et al., The Impact of Stratospheric Ozone on Southern Hemisphere Circulation Change: A Multimodel Assessment, J. Geophys. Res., 115, D00M07, doi:10.1029/2010JD014271, 2010.

SPARC CCMVal: Report on the Evaluation of Chemistry-Climate Models, edited by: Eyring, V., Shepherd, T., and Waugh, D., SPARC Report No. 5, WCRP-30/2010, WMO/TD – No. 40, available at: www.sparc-climate.org/publications/sparc-reports/, 2010

Szopa, S. et al. (2013). Aerosol and ozone changes as forcing for climate evolution between 1850 and 2100. Clim Dyn https://doi.org/10.1007/s00382-012-1408-y

Unger N. & Yue X. Strong chemistry-climate feedback in the Pliocene, Geophys. Res. Lett., 41, 527–533, doi:10.1002/2013GL058773, 2014.

WMO (World Meteorological Organization), Scientific Assessment of Ozone Depletion: 2014, World Meteorological Organization, Global Ozone Research and Monitoring Project-Report No. 55, 416 pp., Geneva, Switzerland, 2014.

Figures

Table 1: Set-up of the simulations

Setup Name	CO_2	CH_4	N_2O	SST	Ozone
PREIND	285 ppm	791 ppb	275 ppb	AMIP	Interactive
EOCENE	1120 ppm	3614 ppb	323 ppb	Extracted from FOAM Eocene simulation	Interactive
EOCENE_OzRoyer					Prescribed from Royer
EOCENE_Oz1855					Prescribed from Szopa et al. (2013)

Clim. Past Discuss., https://doi.org/10.5194/cp-2018-115
Manuscript under review for journal Clim. Past
Discussion started: 24 September 2018

Climate of the Past Discussions
Open Access
EGU

Table 2: Global change of total ozone column, temperature and effective radiative forcings induced by the use of an interactive stratospheric chemistry instead of climatologies.

	Interactive O_3 vs Royer (EOCENE- EOCENE_OzRoyer)	Interactive O_3 vs a 11 year mean climatology centered on 1855 (EOCENE- EOCENE_Oz1855)
Change of globally averaged TOC (DU)	45.5	34.2
Effective radiative forcing ($W.m^{-2}$)	1.4	1.7
Global Temperature change (K)	0.4	0.3
Stratospheric temperature change (K) above 230 hPa	1.4	1.

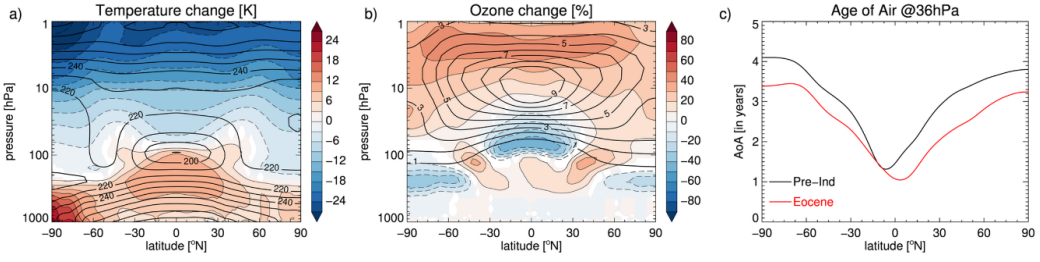

Figure 1: Annual mean differences (EOCENE minus PREIND) of zonally averaged temperature (in K, panel a) and ozone (in %, panel b). Color filled contours indicate that anomalies are statistically different at the 1% confidence level according to a t-test. Black contours show the preindustrial climatology. Zonally averaged age of air (in years, panel c) at 36 hPa in the EOCENE (red) and PREIND (black) simulations.

Clim. Past Discuss., https://doi.org/10.5194/cp-2018-115
Manuscript under review for journal Clim. Past
Discussion started: 24 September 2018

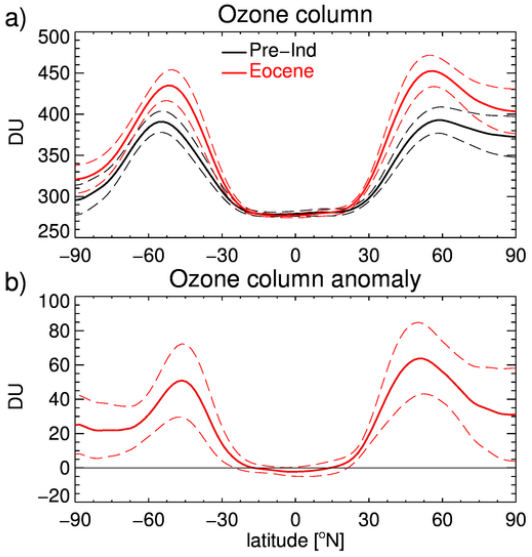

Figure 2: Latitudinal profile of the total ozone column (in Dobson Unit or DU, panel a) in the (red) EOCENE and (black) PREIND simulation. Total ozone column change (in DU, panel b) between the EOCENE and PREIND simulation. Dashed lines delimit the 2-σ uncertainty envelop, which is represented by the standard error of the mean.

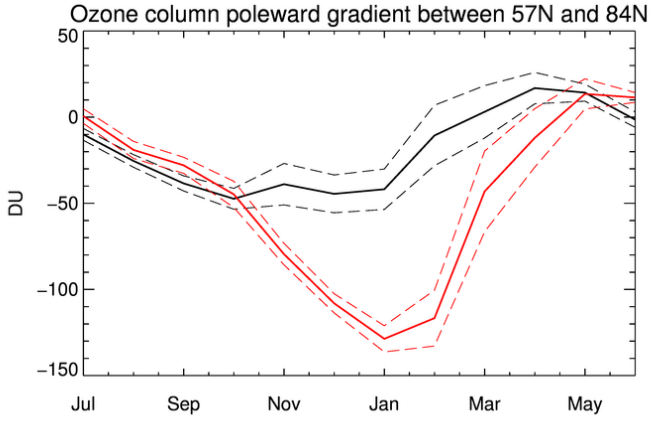

5

Clim. Past Discuss., https://doi.org/10.5194/cp-2018-115
Manuscript under review for journal Clim. Past
Discussion started: 24 September 2018

Climate of the Past Discussions
Open Access
EGU

Figure 3: Zonally averaged seasonal evolution of the latitudinal gradient (computed as the difference between 84° N and 57° N) of the total ozone column for the EOCENE (red) and PREIND (black) simulations. Dashed lines delimit the 2-σ uncertainty envelope, which is represented by the standard error of the mean.

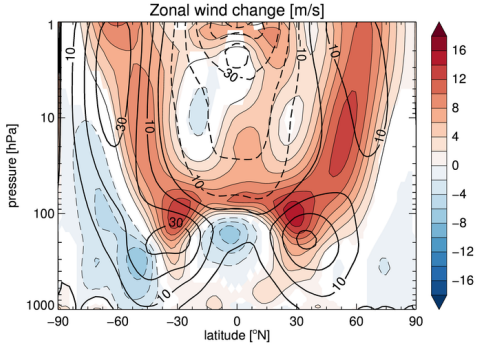

Figure 4: Annual mean differences (EOCENE minus PREIND) of zonally averaged zonal wind (in m/s). Color filled contours indicate that anomalies are statistically different at the 1% confidence level according to a t-test. Black contours show the preindustrial climatology.

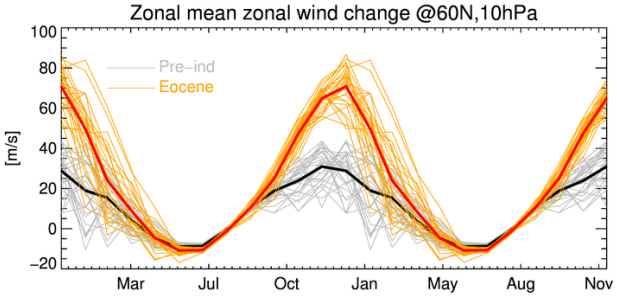

Figure 5: Time series of the monthly mean zonal-mean zonal wind at 60° N and 10 hPa (~31 km) for the Eocene and preindustrial simulations. Red and black curves show the climatological averages for the Eocene and Preindustrial simulations, respectively. All simulated years are individually plotted in thin yellow (EOCENE) and grey (PREIND). Note that each year is repeated twice to visualize better the seasonal cycle.

Clim. Past Discuss., https://doi.org/10.5194/cp-2018-115
Manuscript under review for journal Clim. Past
Discussion started: 24 September 2018

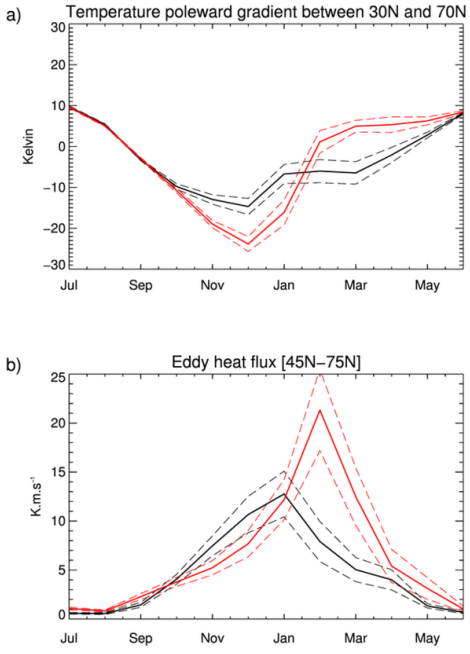

Figure 6: As Figure 2 but for (a) the zonal-mean temperature poleward gradient calculated between 30° N and 70° N at 10 hPa (~32 km), and (b) the eddy heat flux averaged in the latitudinal band [45,75]° N at 100 hPa (~16 km).

5

Clim. Past Discuss., https://doi.org/10.5194/cp-2018-115
Manuscript under review for journal Clim. Past
Discussion started: 24 September 2018

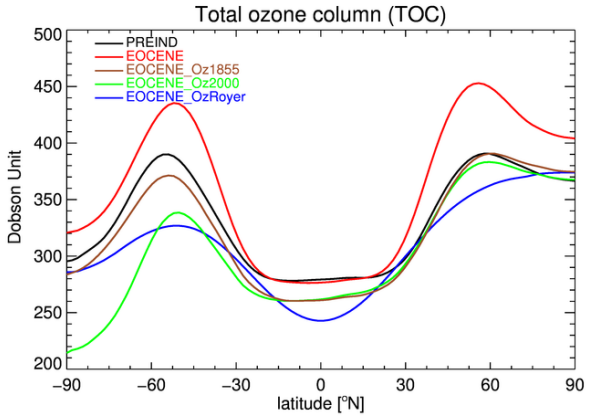

Figure 7: Latitudinal distribution of ozone considered by the circulation model LMDz when using climatologies from Royer (blue), from Szopa et al. (2013) centered on the year 2000 (green) or centered on the year 1855 (maroon), or interactively computed by REPROBUS for Eocene conditions (red) or preindustrial conditions (black).

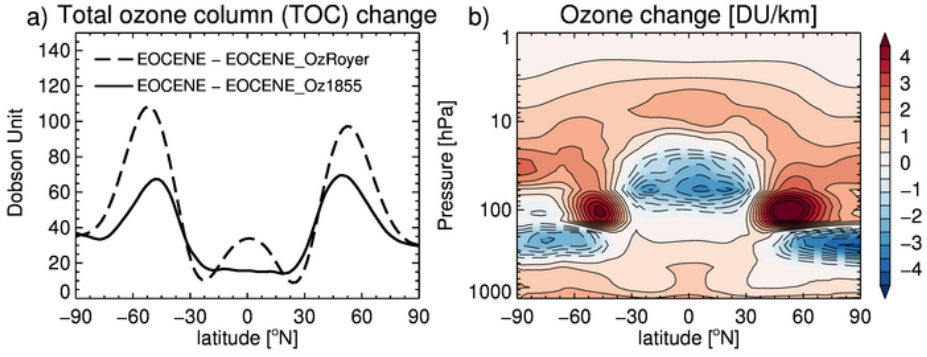

Figure 8: Total ozone column (TOC) changes (in Dobson Units or DU) between the EOCENE simulation and the EOCENE-Oz1855 simulation (considering the 1855 ozone climatology) (panel a), and TOC changes between the EOCENE simulation and the two climate-only simulations considering the (solid) 1855 ozone climatology and (dashed) Royer ozone parameterization (panel b).

Clim. Past Discuss., https://doi.org/10.5194/cp-2018-115
Manuscript under review for journal Clim. Past
Discussion started: 24 September 2018

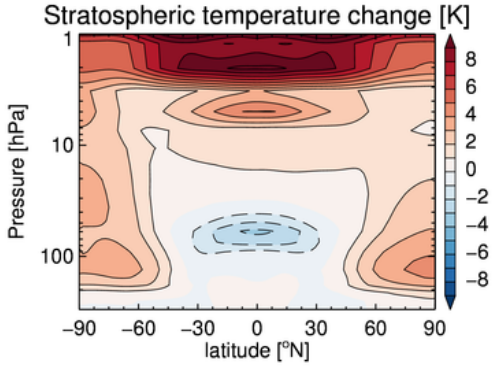

Figure 9: Stratospheric temperature changes (K) between the EOCENE simulation and the climate-only simulation with the 1855 ozone climatology.